Kobe University Repository : Kernel

PDF issue: 2026-07-14

Screening to isolate Bacillus subtilis mutants with enhanced NADPH levels

Wu, Yuzheng
Ishikawa, Shu
Yoshida, Ken-ichi

(Citation)
The Journal of General and Applied Microbiology,70(5):205-211

(Issue Date)
2024

(Resource Type)
journal article

(Version)
Version of Record

(Rights)
© 2024 Applied Microbiology, Molecular and Cellular Biosciences Research Foundation
This article is licensed under a Creative Commons [Attribution-NonCommercial-NoDerivatives 4.0 International] license.

(URL)
https://hdl.handle.net/20.500.14094/0100497258

J. Gen. Appl. Microbiol., **70**, 205–211 (2024)
doi 10.2323/jgam.2025.01.001
©2024 Applied Microbiology, Molecular and Cellular Biosciences Research Foundation

jGAM

Full Paper

Screening to isolate *Bacillus subtilis* mutants with enhanced NADPH levels

(Received December 12, 2024; Accepted January 6, 2024; J-STAGE Advance publication date: January 16, 2025)

Yuzheng Wu, Shu Ishikawa, and Ken-ichi Yoshida*

Department of Science, Technology and Innovation, Kobe University, 1-1 Rokkodai, Nada, Kobe 657- 8501, Japan

As the first step toward understanding how NADPH levels are regulated in *Bacillus subtilis*, we sought to obtain mutant strains with enhanced NADPH levels. Our previous study demonstrated that in a strain of *B. subtilis* expressing bacterial luciferase derived from *Photorhabdus luminescens*, artificially enhancing NADPH levels enhanced luciferase luminescence in the colonies. In this study, from a library of ethyl methanesulfonate-treated mutants, those with enhanced luciferase luminescence in colonies were isolated, and five isolates were further selected by luminescence in microplate culture. Finally, we measured intracellular NADPH levels of them and found that all the five strains had significantly enhanced NADPH levels compared to the parental strain. In addition, four strains significantly increased total NADP(H) levels. These results demonstrate the effectiveness of our strategy as a methodology for obtaining mutant strains useful for elucidating the mechanisms for regulation of NADPH levels in *B. subtilis*.

Keywords: *Bacillus subtilis*; luciferase; NADPH

Introduction

Reduced nicotinamide adenine dinucleotide phosphate (NADPH) is a critical anabolic electron donor across all organisms, including eukaryotes, bacteria, and archaea. It plays a dual role. On the one hand, NADPH is used to generate reactive oxygen species (ROS) and maintaining organisms' antioxidative defense systems (Schröder, 2019). More significantly, it provides the driving reducing power for numerous biosynthetic enzymatic reactions, including those responsible for producing essential cellular components like DNA, RNA, and lipids (Aliverti et al., 2021). Due to its central role in biosynthesis, NADPH availability has garnered significant interest in industrial applications. Many valuable natural products, particularly complex secondary metabolites, are synthesized through processes that heavily rely on NADPH-dependent enzymes (Spaans et al., 2015). Thus, the involvement of NADPH in vital biological processes and its importance in biosynthesis underscore its essentiality as a molecule.

The oxidative pentose phosphate pathway (oxPPP), the Entner–Doudoroff (ED) pathway, and the isocitrate dehydrogenase step in the tricarboxylic acid (TCA) cycle have traditionally been recognized as the primary sources of NADPH (Sauer and Eikmanns, 2005). However, more research indicates the significance of other NADPH-generating enzymes, including transhydrogenases (Sauer et al., 2004; Ragland et al., 1966), glucose dehydrogenases (Ragland et al., 1966), and non-phosphorylating glyceraldehyde 3-phosphate dehydrogenases (GAPN) (Habenicht, 1997). In *Escherichia coli* and many other bacterial species, an $NAD(P)^+$ transhydrogenase utilizes NADH to reduce $NADP^+$ to NADPH, which balances the interconversion of NADH and NADPH. However, in *Bacillus subtilis*, no typical gene encoding this enzyme has been identified within its genome, although some studies have reported potential $NAD(P)^+$ transhydrogenase activity (Rühl et al., 2012). When the *E. coli pntAB* genes, which encode the $NAD(P)^+$ transhydrogenase, were expressed in a *B. subtilis* cell factory engineered for converting *myo*-inositol into *scyllo*-inositol, the conversion efficiency was improved slightly but significantly (Tanaka et al., 2017). These results suggest that the introduced *E. coli* $NAD(P)^+$ transhydrogenase could increase NADPH availability in *B. subtilis*.

The mechanism and regulation for endogenous NADPH regeneration in *B. subtilis* remains poorly understood. We could speculate that some reactions in central metabolic pathways, such as gluconeogenesis, oxPPP, and TCA cycle, may contribute to NADPH regeneration. In gluconeogen-

*Corresponding author: Ken-ichi Yoshida, Department of Science, Technology and Innovation, Kobe University, 1-1 Rokkodai, Nada, Kobe 657-8501, Japan.
Phone/Fax: +81-78-803-5891 E-mail: kenyoshi@kobe-u.ac.jp

None of the authors of this manuscript has any financial or personal relationship with other people or organizations that could inappropriately influence their work.

esis, a malic enzyme encoded by *ytsJ* is capable of regenerating NADPH. However, in the subsequent reaction, glyceraldehyde 3-phosphate dehydrogenase encoded by *gapB* consumes NADPH, making it unlikely for gluconeogenesis to be a net source of NADPH. In contrast, oxPPP could offer at least two reactions that generate NADPH; one is catalyzed by Zwf (glucose 6-phosphate dehydrogenase) and the other by GndA (6-phosphogluconate dehydrogenase) (Lim et al., 2002; Rippa et al., 1998). Additionally, in TCA cycle, Icd (isocitrate decarboxylase) could also regenerate NADPH. Among the enzymes for these reactions involving the regeneration of NADPH, CcpA and CcpC regulate the expression of *icd* under carbon catabolite repression, and *ytsJ* is controlled by LexA and induced upon DNA damage. On the other hand, *zwf* and *gndA* are constitutively expressed, with no known regulatory mechanisms reported. Despite these findings, in *B. subtilis* the enzyme primarily responsible for NADPH regeneration remains unknown. Nonetheless, limited availability of NADPH due to insufficient regeneration rate often results in cellular vulnerability to elevated levels of ROS, potentially leading to cell death. These limitations also hinder the efficient production of high-value chemicals that demand significant quantities of this cofactor. Enhancing NADPH availability has remained a significant challenge in metabolic engineering (Ding et al., 2024; Lee et al., 2013; Fuhrer and Sauer, 2009).

Bacterial luciferase depends on a cascade reaction catalyzed by a series of enzymes encoded by the *luxABCDE* operon. LuxA and LuxB are the respective α- and β-subunits of luciferase. LuxC, LuxD, and LuxE constitute the fatty acid reductase complex to synthesize the long-chain fatty aldehyde with consumption of NADPH and ATP. The luciferase reaction is an oxidative process as molecular oxygen oxidizes $FMNH_2$ and the long-chain fatty aldehyde to the corresponding acid. The reaction forms an excited intermediate, which oxidizes $FMNH_2$ into FMN to emit blue-green light. NAD(P)H-dependent FMN reductases are common in many bacterial species, including *E. coli* and *B. subtilis*, and the reduction of FMN into $FMNH_2$ depends on NAD(P)H availability. Therefore, the bioluminescence of bacterial luciferase depends on NAD(P)H levels (Gupta et al., 2003; Kaku et al., 2021; Wu et al., 2022). In a previous study, we created a luciferase monitoring system based on the *lux* genes derived from *Photorhabdus luminescens* (Gupta et al., 2003). The *gdh* of *B. subtilis* encodes a sporulation-specific glucose dehydrogenase dependent on NADP(H). When *gdh* was expressed constitutively in growing cells, intracellular NADPH increased significantly (Xu et al., 2007), and the elevated luciferase luminescence was detected as the luminescence intensity of colonies, indicating enhanced cellular NADPH levels (Wu et al., 2022). Thus, the luciferase monitoring system enables us to select colonies of mutants with possible enhanced NADPH levels.

Ethyl methanesulfonate (EMS) is a mutagen often employed for genetic studies. It has a high frequency of causing random point mutations through alkylation of DNA, particularly by converting guanine into O6-ethylguanine that mispairs with thymine (Deng et al., 2023; Khattab and Bazaraa, 2005). This function drives a cascade of G to A transitions, leading to genetic diversity for studying gene function and mutational effects. In this study, we employed EMS to mutagenize the *B. subtilis* strain with the luciferase monitoring system to select mutant strains with higher luciferase luminescence in a stepwise fashion and determined the intracellular NADPH levels to isolate mutant strains with enhanced NADPH levels. Thus, this study provides a milestone in our quest to unravel the mechanism of the NAPDH supply in *B. subtilis*.

Materials and methods

Bacterial strains and culture conditions. Strains of *B. subtilis*, listed in Table 1, were maintained on Lennox Broth (LB) agar plates (2% w/v Lennox LB, Difco) at 37°C. The culture media were supplemented with antibiotics as required: 0.5 μg/mL erythromycin (Fujifilm) and 100 μg/mL spectinomycin (Fujifilm). For the experimental conditions, main cultures of the bacteria were diluted in 200 mL of 4% soytone broth, composed of 4% Bacto soytone (Difco), 0.5% Bacto Yeast Extract (Difco), and 0.2% glucose, in a 500 mL baffled flask to the optical density for cells at 600 nm (OD_{600}) of 0.05 and allowed to grow at 37°C with shaking at 200 rpm.

Determination of NADP(H) concentrations. Strains of *B. subtilis* were grown in 4% soytone broth at 37°C with shaking for 19 h. The intracellular NADPH concentrations were determined on the collected cells using the EnzyChrom™ NADP/NADPH Assay Kit as instructed by

Table 1. Bacterial strains used in this study.

Strain	Genotype	Source or reference
B. subtilis		
168	*trpC2*	Laboratory stock
KU302	*amyE*::(P*rpsO-iolG-iolW-iolT cat*) Δ*iolABCDEF* Δ*iolHIJ* Δ*iolX* Δ*iolR trpC2*	Tanaka et al., 2017
KW028	*aprE*::(P*spac-gdh spc*) *sacA*::(P*yhaM-luxABCDE erm*) on the KU302 background	Wu et al., 2022
WY002	*sacA*::(P*yhaM-luxABCDE erm*) on the KU302 background	Wu et al., 2022
M1-1	A mutant strain of WY002	This study
M1-2	A mutant strain of WY002	This study
M1-3	A mutant strain of WY002	This study
M1-11	A mutant strain of WY002	This study
M1-17	A mutant strain of WY002	This study

the supplier (BioAssay Systems). The intracellular concentration of NADPH was calculated assuming that 1 OD_{600} unit corresponded to 10^9 cells and that each cell had a volume of 1.41 μm^3 (Kubitschek, 1969).

EMS mutagenesis. Strain WY002 [*sacA*::(P*yhaM-luxABCDE erm*) on KU302 background] was inoculated onto LB plates and incubated at 30°C for 18 h. Then, a fresh colony was inoculated into LB to OD_{600} of 0.05 and allowed to grow at 37 °C with shaking at 200 rpm. After about 3 h, when OD_{600} became 0.5, cells were harvested and suspended into 10 mL of LB containing 0, 100, or 200 mM EMS at 37°C with shaking at 200 rpm for 30 min. Cells were washed twice with 5 mL of LB and resuspended and incubated at 37°C for 30 min. Then, the cell suspension was diluted appropriately, spread on 4% soytone plates, and incubated at 37°C overnight. Luciferase luminescence of colonies on the plates was scanned as described below.

Luciferase assays. The luminescence of colonies was quantified and normalized as follows. The liquid culture of *B. subtilis* was diluted to give about 1,000 colony-forming units, 1 mL of which was spread on each of 4% soytone agar plates in a rectangular petri dish (140×100×14.5 mm) and incubated at 37°C for 11 h to form about 1,000 colonies. The plate was set in a ChemiDoc XRS+ (Bio-Rad) under Chemi Hi Resolution conditions with a fixed exposure time of 90 s to capture the luminescence reversal image of the entire plate. The images were analyzed using ImageJ to quantify luminescence intensity [integrated density (IntDen)] for each colony (Wu et al., 2022).

Strains of *B. subtilis* were grown on LB plates at 37°C overnight. Cells in freshly formed colonies were inoculated into 2 mL of LB to make an OD_{600} of 0.05 and allowed to grow for 5 h at 37°C with shaking at 200 rpm. The cultures were diluted in 4% soytone broth to make an OD_{600} of 0.05, and their aliquots (100 μl each) were dispensed into a 96-well microtiter plate, which is set in Cytation™ 5 Cell Imaging Multi-Mode Reader (Agilent). The bacteria were incubated at 37°C for 24 h with the shaking function equipped with the reader. During the growth, the luminescence of luciferase and OD_{600} in each well were monitored simultaneously over time. The luminescence [relative light unit (RLU)] was normalized by OD_{600} as expressed as RLU/OD_{600}.

Results

Conditions to isolate mutants with high luciferase luminescence by EMS mutagenesis

In a previous study, we created a luciferase monitoring system in *B. subtilis* by introducing the *lux* genes derived from *Photorhabdus luminescens* (Gupta et al., 2003) to generate strain WY002 [*sacA*::(P*yhaM-luxABCDE erm*) on the KU302 background] (Table 1), which allows us to monitor the NAD(P)H without disrupting the cells. We also made strain KW028 [*aprE*::(P*spac-gdh spc*) *sacA*::(P*yhaM-luxABCDE erm*) on the KU302 background], which possesses *gdh* for glucose dehydrogenase enabling the artificial supply of NADPH. This strain was utilized as a positive control to confirm that the luciferase luminescence of the colony is enhanced by elevated NADPH levels.

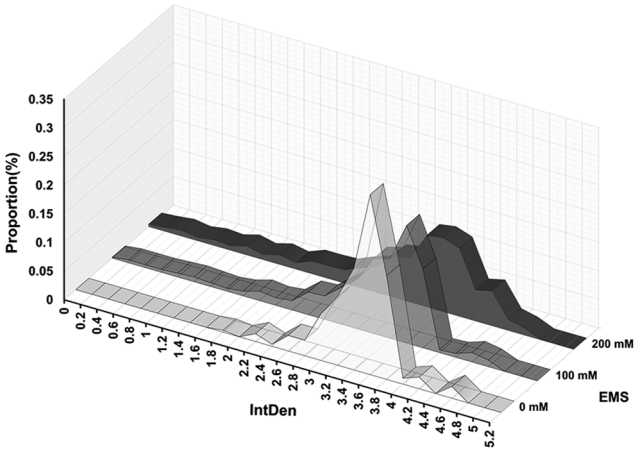

Fig. 1. Distribution of luciferase luminescence intensities (IntDen) of *B. subtilis* colonies formed on the plates after EMS treatment.

Strain WY002 was treated with the given EMS concentrations for 30 min and then spread on each plate to form about 1,000 colonies. The IntDen values of the colonies were calculated and the distribution histograms of the values are shown.

We treated WY002 with EMS to induce mutations. It can produce high-frequency point mutations and is employed for random mutagenesis. Considering that a higher concentration of EMS will result in a larger number of mutations, we set two concentrations of EMS, 100 and 200 mM, for a 30-min exposure to investigate how the distribution of luminescence intensity of the emerging colonies changes compared to that of the colonies without EMS treatment (0 mM). After 30-min exposure to 100 mM and 200 mM EMS, approximately 50% and 10% of cells can survive, respectively.

After the EMS treatment, the luminescence of luciferase of about 1,000 colonies that appeared on the plates was captured to generate the reversal images. The images were analyzed to quantify the luminescence intensity of each of the colonies. Thus, the histograms were generated to display the distribution for colonies with different luminescence intensities under different mutagenesis conditions (Fig. 1). As the EMS concentration was elevated, the proportion of colonies with higher and lower luminescence increased. On the other hand, the percentage of IntDen 3.6-3.8 colonies, the most numerous in the luminescence intensity distribution, decreased in a stepwise manner. These results suggested that EMS treatment caused some mutation that altered the luciferase luminescence intensity of the colonies. Therefore, as the first round of mutant selection, we repeated the mutagenesis in conditions with 200 mM EMS for 30 min and then selected the colonies with the highest luminescence intensity as the candidates for the desired mutant strains.

Selection of candidate mutant strains with enhanced luciferase luminescence

After the first round of selection described above, we obtained 167 candidates exhibiting higher luciferase luminescence. Each of the candidates was pricked on new plates

to make four replicated colonies at 37°C for 3 h, and the luminescence of them was captured to generate the image files. Processing the image files, we calculated the IntDen value for the colonies of each candidate. In addition, each of the candidates was inoculated into 4% soytone broth and allowed to grow at 37°C in a microtiter plate with shaking to monitor OD_{600} and luciferase luminescence continuously over time for 24 h.

Thus, we selected out the five final isolates designated as M1-1, M1-2, M1-3, M1-11, and M1-17, which exhibited the significantly enhanced IntDen values (Table 2). M1-1, M1-2, and M1-3 grew almost similarly to the parental strain WY002 and the positive control KW028 (Fig. 2).

Table 2. Luciferase luminescence intensities of colonies of strains of *B. subtilis*.

Strain	Luciferase luminescence intensities (IntDen) [a]
WY002	2.262 ± 0.365
KW028	2.532 ± 0.138*
M1-1	3.595 ± 0.090**
M1-2	3.625 ± 0.099**
M1-3	3.392 ± 0.320**
M1-11	3.333 ± 0.381**
M1-17	3.764 ± 0.104**

[a] Values are the means ± SD of the IntDen of four replicated colonies. Significant differences for the value of WY002 by Student's t-test are shown: *, $0.01 < P < 0.05$, and **, $P < 0.01$.

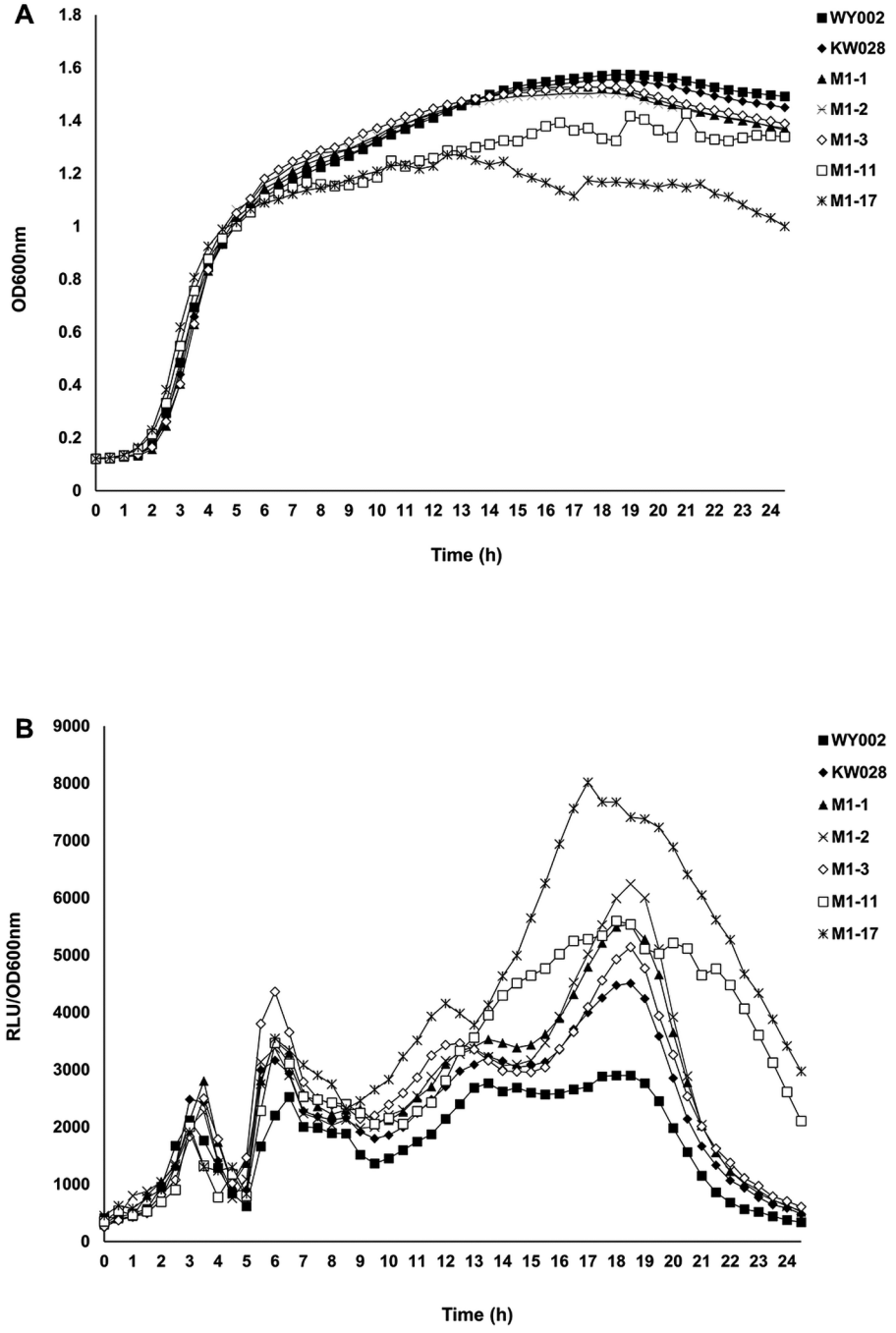

Fig. 2. Growth curves (A) and luciferase luminescence in liquid cultures (B) of strains of *B. subtilis*. Growth curves are expressed as the logarithmic change in OD_{600} over time. The luciferase luminescence is the value of RLU/OD_{600}. A representative data set is shown after three independent experiments.

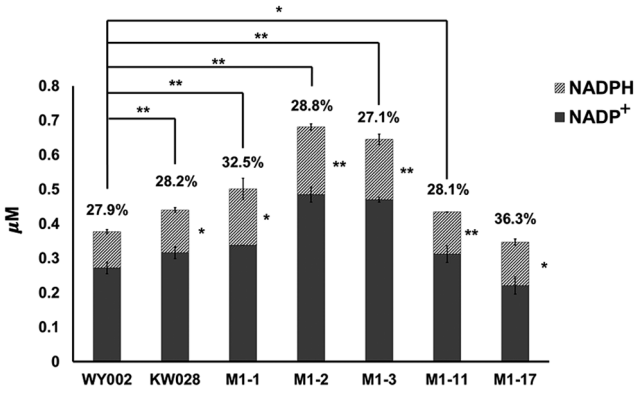

Fig. 3. The NADP(H) levels of strains of *B. subtilis*.

The levels of $NADP^+$ and NADPH in the cells are shown in stacked bar graphs. The values are means ± SD of the results from three independent measurements. For NADPH and total NADP(H) levels, significant differences from WY002 by Student's t-test are shown: *, $0.01 < P < 0.05$, and **, $P < 0.01$. The percentage of [NADPH]/[total NADP(H)] is presented on each bar.

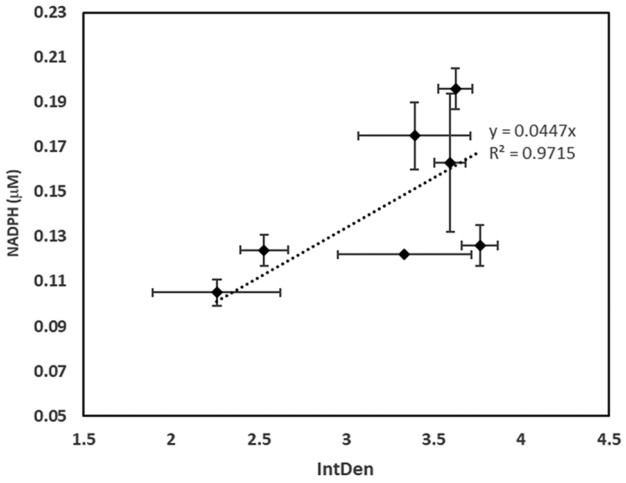

Fig. 4. The correlation between the luminescence intensity of the colonies and the NADPH concentration of strains of *B. subtilis*.

The luminescence intensity of the colonies in Table 2 and the NADPH concentration in Fig. 3 were plotted to calculate the regression curve as indicated.

On the other hand, M1-11 and M1-17 showed relatively poor growth. The intensity of luciferase luminescence generally exhibited a typical curve of elevation after the stationary phase, with WY002 luminescence being the lowest, followed by KW028, and all the candidate strains exhibited much higher intensity. Since biomass synthesis is suppressed during the stationary phase, it is presumed that the surplus NADPH can be available for luciferase luminescence.

Enhanced NADPH levels of the mutants

The five candidates with WY002 and KW028 underwent the determination of NADP(H) concentrations (Fig. 3). The positive control KW028 showed an elevated NADPH level as the cause of its enhanced luciferase luminescence. All the candidates exhibited significantly enhanced NADPH levels compared with the parental strain WY002. M1-2, M1-3, and M1-11 accumulate higher levels of NADPH compared to KW028, in which the *gdh* gene was artificially introduced. On the other hand, all but M1-17 had increased total NADP(H) than WY002. Although these results were unexpected, the increase in NADPH levels may have triggered the induction of $NADP^+$ biosynthesis.

The correlation between the luminescence intensity of the colonies in Table 2 and the NADPH concentration in Fig. 3 was examined (Fig. 4). The results indicated a positive correlation between luciferase luminescence intensity and intracellular NADPH concentration. Thus, the validity of our screening strategy to select mutants with enhanced NADPH levels based on luciferase luminescence intensity was assured.

Discussion

The results of this study highlight the potential of combining chemical mutagenesis with high-throughput luminescence screening as a powerful tool for revealing uncharacterized gene function and regulation for enhanced NADPH levels, which is necessary to drive future metabolic engineering. EMS mutagenesis is a random gene mutation and is extremely useful for creating diverse mutant libraries. It is also clear that our system, which allows us to assess luciferase luminescence levels by image analysis of colonies, as well as automated dual monitoring of luciferase activity and cell concentration over time in microculture, provides a highly sensitive method for identifying desirable mutants. In particular, because the luminescence intensity of the colonies varied so widely, the microculture was effective in narrowing down the 167 candidates to the final five. Our ability to accurately identify the five mutants with enhanced NADPH regeneration, obtained for the first time, is remarkable. Mutants with significantly increased NADPH levels may have mutations in pathways directly or indirectly related to NADPH regeneration. We plan to sequence the entire genomes of these mutants to reveal what enzymes or reaction pathways are responsible for the enhanced NADPH levels. However, tremendous experimentation will be required to elucidate them, and this study has a significance as a milestone on the long road ahead.

On the other hand, our strategy has some weaknesses as well. Strain WY002, the subject of EMS mutagenesis, has the gene set for luciferase system, and the mutation can also occur in these genes. Although some mutations could result in stronger luminescence, it is more likely that most mutations result in weaker luminescence or no activity at all. In fact, the proportion of colonies with weakened luminescence appeared to increase when treated with high concentrations of EMS (Fig. 1). From this point of view, our strategy is suitable for selecting for increased luminescence intensity but not for weakened ones. In addition, EMS mutagenesis is inherently random and may result in mutations that adversely affect other cellular processes than NADPH regeneration. In this study, EMS mutagenesis resulted in several hundred thousand colonies, which means that all of them should grow normally. Nevertheless, two of the five final isolates showed reduced growth in

microculture (Fig. 2). Whether the observed reduced growth can be a phenotype directly related to enhanced NADPH levels remains to be clarified. However, it may be possible that some anabolic pathways for growth that utilize NADPH were impaired, and NADPH was unconsumed to increase a surplus of NADPH in these mutants. It is also considered that the luciferase system consumes intracellular energy, which could confound the results under certain metabolic conditions.

It was surprising that the intracellular NADP(H) pool increased in four of the isolates (Fig. 3). Certainly, a change in the internal environment in the form of an increase in the level of NADPH results in a decrease in the level of $NADP^+$. However, in actual measurements, $NADP^+$ is not depleted; about 70% of NADP(H) pool is $NADP^+$. Interestingly, this ratio of $NADP^+$ to NADPH seems to remain nearly constant in all strains. Maintaining this ratio might trigger the induction of NADP(H) biosynthesis. Increasing the overall NADP(H) pool may be a waste of intracellular resources. However, the growth of M1-2 and M1-3 with the most increased pools does not seem to deteriorate markedly. Rather, a deterioration in growth was observed in M1-11 and M1-17, where the pool was slightly elevated and reduced compared to the parental strain, but the NADPH level increased. Therefore, it is more important to maintain the ratio of $NADP^+$ to NADPH, and it is possible to consider that in order to increase the NADPH level, $NADP^+$ increased accordingly, resulting in an increase in NADP(H) pool.

The significance of increased levels of NADPH goes beyond basic studies; increased NADPH levels are essential for various biotechnological applications, including the production of reduced biochemicals, detoxification of reactive oxygen species, and support of anabolic processes. Our approach could contribute to breeding strains optimized for industrial-scale production of NADPH-dependent products such as pharmaceuticals, biofuels, fine chemicals, etc. The combination of EMS mutagenesis and luciferase-based monitoring systems provides an efficient and scalable strategy to enhance redox balance in cells. Future work could further refine and extend this approach and application to other metabolic pathways and biological production.

Conclusions

In this study, we successfully developed and applied a novel approach for selecting mutants with enhanced NADPH levels using EMS mutagenesis combined with a luciferase luminescent monitoring system. The integration of chemical mutagenesis and luminescent screening allowed for the efficient identification of mutants with significantly improved NADPH production. The identified strains exhibited enhanced NADPH availability, demonstrating the effectiveness of our strategy for optimizing intracellular redox balance. This approach provides a robust platform for strain improvement, which is extendable to other systems requiring high NADPH levels for industrial bioprocesses.

References

Aliverti, A., Faber, R., Finnerty, C. M., Ferioli, C., Pandini, V. et al. (2001) Biochemicala and crystallographic characterization of ferredoxin-NADP(+) reductase from nonphotosynthetic tissues. *Biochemistry*, **40**, 14501–14508.

Deng, L., Wang, C., Zhang, X., Yang, W., Tang, H. et al. (2023) Cell-to-cell natural transformation in *Bacillus subtilis* facilitates large scale of genomic exchanges and the transfer of long continuous DNA regions. *Nucleic Acids Res*., **51**, 3820-3835.

Ding, N., Yuan, Z., Sun, L., and Yin, L. (2024) Dynamic and static regulation of nicotinamide adenine dinucleotide phosphate: strategies, challenges, and future directions in metabolic engineering. *Molecules*, **29**, 3687.

Fuhrer, T. and Sauer, U. (2009) Different biochemical mechanisms ensure network-wide balancing of reducing equivalents in microbial metabolism. *J. Bacteriol.*, **191**, 2112-21.

Gupta, R. K., Patterson, S. S., Ripp, S., Simpson, M. L., and Sayler, G. S. (2003) Expression of the *Photorhabdus luminescens lux* genes (*luxA*, *B*, *C*, *D*, and *E*) in *Saccharomyces cerevisiae*. *FEMS Yeast Res.,* **4**, 305–313.

Habenicht, A. (1997) The non-phosphorylating glyceraldehyde-3-phosphate dehydrogenase: biochemistry, structure, occurrence and evolution. *Biol. Chem*., **378**, 1413-9.

Kaku, T., Sugiura, K., Entani, T., Osabe, K., and Nagai, T. (2021) Enhanced brightness of bacterial luciferase by bioluminescence resonance energy transfer. *Sci. Rep*., **11**, 14994.

Khattab, A. A. and Bazaraa, W. A. (2005) Screening, mutagenesis and protoplast fusion of *Aspergillus niger* for the enhancement of extracellular glucose oxidase production. J. Ind. *Microbiol. Biotechnol.*, **32**, 289-94.

Kubitschek, H. E. (1969) Growth during the bacterial cell cycle: analysis of cell size distribution. *Biophys. J.,* **9**, 792–809.

Lee, W. H., Kim, M. D., Jin, Y. S., and Seo, J. H. (2013) Engineering of NADPH regenerators in *Escherichia coli* for enhanced biotransformation. *Appl. Microbiol. Biotechnol*., **97**, 2761–2772.

Lim, S. J., Jung, Y. M., Shin, H. D., and Lee, Y. H. (2002) Amplification of the NADPH-related genes *zwf* and *gnd* for the oddball biosynthesis of PHB in an *E. coli* transformant harboring a cloned *phbCAB* operon. *J. Biosci. Bioeng.*, **93**, 543-549.

Ragland, T. E., Kawasaki, T., and Lowenstein, J. M. (1966) Comparative aspects of some bacterial dehydrogenases and transhydrogenases. *J. Bacteriol.*, **91**, 236-44.

Rippa, M., Giovannini, P. P., Barrett, M. P., Dallocchio, F., and Hanau, S. (1998) 6-Phosphogluconate dehydrogenase: the mechanism of action investigated by a comparison of the enzyme from different species. *Biochim. Biophys. Acta*., **1429**, 83-92.

Rühl, M., Le Coq, D., Aymerich, S., and Sauer, U. (2012) 13C-flux analysis reveals NADPH-balancing transhydrogenation cycles in stationary phase of nitro-

gen-starving *Bacillus subtilis*. *J. Biol. Chem.,* **287**, 27959-70.

Sauer, U. and Eikmanns, B. J. (2005) The PEP–pyruvate–oxaloacetate node as the switch point for carbon flux distribution in bacteria. *FEMS Microbiol. Rev.,* **29**, 765–794.

Sauer, U., Canonaco, F., Heri, S., Perrenoud, A., and Fischer, E. (2004) The soluble and membrane-bound transhydrogenases *UdhA* and *PntAB* have divergent functions in NADPH metabolism of *Escherichia coli*. *J. Biol. Chem.,* **279**, 6613–6619.

Schröder, K. (2019) NADPH oxidase-derived reactive oxygen species: Dosis facit venenum. *Exp Physiol.*, **104**, 447-452.

Spaans, S. K., Weusthuis, R. A, van der Oost, J., and Kengen, S. W. M. (2015) NADPH-generating systems in bacteria and archaea. *Front. Microbiol*., **6**, 742.

Tanaka, K., Natsume, A., Ishikawa, S., Takenaka, S., and Yoshida, K. (2017) A new-generation of *Bacillus subtilis* cell factory for further elevated *scyllo*-inositol production. *Microb. Cell Fact*., **16**, 67.

Wu, Y., Kawabata, H., Kita, K., Ishikawa, S., Tanaka, K. et al. (2022) Constitutive glucose dehydrogenase elevates intracellular NADPH levels and luciferase luminescence in *Bacillus subtilis*. *Microb. Cell Fact.*, **21**, 266.

Xu, Z., Jing, K., Liu, Y., and Cen, P. (2007) High-level expression of recombinant glucose dehydrogenase and its application in NADPH regeneration. *J. Ind. Microbiol. Biotechnol.*, **34**, 83-90.